Aquaculture 548 (2022) 737720

Contents lists available at ScienceDirect

Aquaculture

journal homepage: www.elsevier.com/locate/aquaculture

Predicting oxygen levels in Atlantic salmon (*Salmo salar*) sea cages

Morten Omholt Alver *, Martin Føre, Jo Arve Alfredsen

NTNU Department of Engineering Cybernetics, 7491 Trondheim, Norway

ARTICLE INFO

Keywords:
Oxygen
Atlantic salmon
Mathematical model
Exposed aquaculture
Advection-diffusion equation

ABSTRACT

Dissolved oxygen (DO) concentration is an important factor affecting fish welfare and growth in Atlantic salmon sea cages. As an operational prediction tool, and to aid our understanding of how DO concentrations are affected by cage size, shape and design interacting with the fish biomass and environmental conditions, we have developed a mathematical model based on the advection-diffusion equation for 3D estimates of DO levels. The model requires input of farm geometry, ambient oxygen levels, current speed and direction, feeding rates, fish distribution and biomass statistics.

The model has been tested for Salmar's Ocean Farm 1, a large production unit dimensioned for 1.5 million fish and designed for coping with exposed environmental conditions, and performs well in comparison with DO measurements, particularly at low to moderate current speeds. Although the model produces realistic outputs with the simple inputs that are available, detailed information about fish behaviour and current conditions within the cage is likely to improve model accuracy.

In addition to being a useful tool for better monitoring of oxygen conditions in fish farms, the present model can, given the appropriate inputs, be used as a forecasting tool for predicting the risk of hypoxic conditions in cages, and to evaluate the risks of hypoxic conditions in new types of open, semi-closed or closed production systems.

1. Introduction

Adequate levels of dissolved oxygen (DO) in salmon sea cages are important to ensure fish welfare and growth, since hypoxia can lead to effects ranging from reduced appetite, stress responses, reduced feed conversion and reduced growth to acute mortality depending on the DO levels encountered (Oppedal et al., 2011; Remen et al., 2013, 2016). Sensors can be used to monitor DO levels, but DO can vary widely throughout the cage volume, as well as over time, rendering a full overview of the status of a cage difficult to obtain through sensors alone (Johansson et al., 2006, 2007; Burt et al., 2012; Solstorm et al., 2018). The distribution of DO levels within a fish cage depends on ambient DO levels, which may vary seasonally and with depth if the water column is stratified. Other key factors affecting DO distribution include cage size and shape, the flow rate and the flow patterns through the cage, and the oxygen consumption by the fish. Oxygen consumption will typically be spatially distributed over the cage volume, and depends on the consumption of individual fish and the stocking density and spatial distribution of fish. Individual oxygen consumption in turn depends on the size and activity level of the fish, its digestion activity (Forsberg, 1997) and the water temperature. The oxygen consumption can be estimated using a model such as the one by Grøttum and Sigholt (1998), although that model doesn't take the variable effect of digestion into account.

For Atlantic salmon, DO levels below 6 mg l^{-1} may considered hypoxic (Burt et al., 2012), although recent research shows that the threshold for hypoxic conditions actually increases with increasing temperature (Remen et al., 2016). The risk of hypoxic conditions in a sea cage is greatest at high temperatures, since increases in temperature leads to a dual effect where the oxygen consumption of the fish increases while the saturation level for DO in seawater decreases. High temperature combined with low current speed leading to low water exchange can therefore lead to low DO levels in parts of the cage. To predict when and where hypoxic conditions can arise, we need to combine our knowledge of (1) the advective and diffusive transport of oxygen across the cage boundaries and through the cage volume, (2) the oxygen consumption by individual fish, and (3) the spatial distribution of the fish.

When introducing new types of production units with larger volumes and larger biomass, or semi-closed or closed concepts, particular attention needs to be paid to the risk of hypoxic conditions. Salmar's Ocean Farm 1 (OF1) is an example of a large open cage system designed

* Corresponding author.
E-mail addresses: morten.alver@ntnu.no (M.O. Alver), martin.fore@ntnu.no (M. Føre), jo.arve.alfredsen@ntnu.no (J.A. Alfredsen).

https://doi.org/10.1016/j.aquaculture.2021.737720
Received 11 May 2021; Received in revised form 11 November 2021; Accepted 13 November 2021
Available online 17 November 2021

for higher biomass and more exposed environmental conditions than regular sea cages. Since evidence suggests that larger units may be more susceptible to hypoxic conditions (Oldham et al., 2018), OF1's large size and biomass capacity warrants extra caution. OF1 is highly instrumented, featuring sensors for temperature, current speed and DO as well as echosounders giving information about the spatial distribution of fish. An extensive open report has been written to document the production system and results of the first production cycle (Myrebøe, 2019).

In this study, we apply an advection-diffusion model coupled with an empirical model of individual oxygen consumption (Grøttum and Sigholt, 1998) and a model of feed distribution and fish feeding behaviour (Alver et al., 2004, 2016) to model DO levels in 3D. The purpose of the model is to predict DO concentrations in the whole cage volume based on the fish biomass and measurable environmental conditions, and thus provide information enabling the assessment of the risk of encountering hypoxic conditions. Combined with measurements, the model can be used as an operational tool to manage and reduce this risk. The model is tested using input values and observations from OF1 over several time periods.

2. Materials and methods

2.1. Mathematical model

To estimate the 3D distribution of DO in sea-cages, we need to combine a model of the physical advection-diffusion processes transporting oxygen through the cage volume with a model describing the oxygen consumption of the fish. The latter model needs to account for the distribution of the fish, which in turn is strongly affected by feeding. It therefore includes a model of the fish population and the feed distribution in the cage that was based on the model of Alver et al. (2016). This model can then in combination with a measure of individual oxygen consumption yield an estimate of the total oxygen consumption of the population. We will in the following describe the DO model and how oxygen consumption is calculated based on the fish and feed model. Symbols used for model inputs, state variables and parameters are summarized in Table 1.

2.1.1. Advection and diffusion of DO

The state variable $\omega(x, y, z, t)$ represents the concentration of dissolved oxygen in mg/l. It is defined in a 3D coordinate system where x is the north-south axis (positive towards the north), y is the east-west axis (positive towards the east) and z is the vertical axis (positive downwards). The time t is given in seconds. The advection-diffusion equation describes the dynamics of $\omega(x, y, z, t)$:

$$\frac{\partial \omega}{\partial t} + v_x\frac{\partial \omega}{\partial x} + v_y\frac{\partial \omega}{\partial y} + v_z\frac{\partial \omega}{\partial z} + \kappa_h\left(\frac{\partial^2 \omega}{\partial x^2} + \frac{\partial^2 \omega}{\partial y^2}\right) + \kappa_v\left(\frac{\partial^2 \omega}{\partial z^2}\right) = \alpha - \sigma \tag{1}$$

where $v_x(x, y, z, t)$, $v_y(x, y, z, t)$ and $v_z(x, y, z, t)$ give the horizontal and vertical components of the current vector, κ_h and κ_v are the horizontal and vertical diffusion coefficients for DO, $\alpha(x, y, z, t)$ the addition rate of oxygen and $\sigma(x, y, z, t)$ the oxygen consumption rate.

If diffusors are used to actively add oxygen within the cage, this can be represented by α values above 0, but in this study $\alpha = 0$ everywhere since we assume no oxygen addition. The oxygen consumption rate $\sigma(x, y, z, t)$ is calculated based on a model for individual oxygen consumption combined with assumptions on the spatial distribution of fish (Section 2.1.2).

Although the rate of molecular diffusion of oxygen is small enough to be neglected on the scale of a salmon cage, the diffusion coefficients κ_h and κ_v are needed to represent the effects of horizontal and vertical turbulent mixing. Generally in the ocean, the rate of horizontal mixing depends on the properties of the flow field, and will typically be higher when there are strong currents and an irregular flow field (e.g. Smagorinsky, 1963). Vertically, the rate of mixing depends on the vertical variability of the current speed and the stability of the water column. Inside of a fish cage, both the cage itself and the movements of the fish can potentially influence the rate of turbulent mixing (Jónsdóttir et al., 2021). These parameters are therefore expected to be dependent on environmental conditions, and are difficult to estimate *a priori*.

For our study, we want to define a reasonably simple model that can be applied to variable environmental conditions. We therefore choose to set $\kappa_h = \kappa_v$, and their value proportional to the square of the current speed:

$$\kappa_h(t) = \kappa_v(t) = 10(v_x(t)^2 + v_y(t)^2) \tag{2}$$

2.1.2. Oxygen consumption

An empirical model for oxygen consumption of Atlantic salmon (mg/kg/h) was derived by Grøttum and Sigholt (1998). Omitting the standard deviations of the model coefficients and changing the time unit to seconds, their equation is as follows:

$$V_{O_2} = 0.0171W^{-0.33}1.03^T1.79^U \tag{3}$$

where W is body weight (kg), T is water temperature (°C) and U is swimming speed (body lengths per second). A study of the sustained swimming capacity of Atlantic salmon by Hvas and Oppedal (2017) gave oxygen consumption rates that were about 30% higher than predicted by the model of Grøttum and Sigholt (1998) at the lowest swimming speed tested (2.2 body lengths s^{-1}), which could be an indication that the Grøttum and Sigholt (1998) model underestimates the oxygen consumption of today's farmed salmon. To compensate for this, we add 30% to the oxygen consumption rate predicted by the Grøttum and Sigholt (1998) model.

The fish are represented in the same way as in the model of Alver et al. (2004, 2016), with the population assumed to have normally distributed individual body weights with mean W_{mean} and standard deviation W_{std} that are kept constant through each simulation. The population is divided into M groups, where each group is defined by a number of individuals (N_k for group k) and mean individual body weight (W_k for group k), resulting in a weight distribution of the population.

For group k, the oxygen consumption rate per kg, $V_{O_2,k}(t)$, is calculated according to Eq. (3). The group's contribution to $\sigma(x, y, z, t)$ is denoted $\sigma_k(x, y, z, t)$ and found as follows:

$$\sigma_k(x, y, z, t) = V_{O_2,k}(t)N_kW_k\beta(x, y, z, t) \tag{4}$$

where $\beta(x, y, z, t)$ is the relative distribution of the fish over the cage volume (see Section 2.1.3). The total oxygen consumption rate is thus found as:

$$\sigma(x, y, z, t) = \sum_{k=1}^{M}\sigma_k(x, y, z, t) \tag{5}$$

2.1.3. Spatial distribution of fish

Feeding affects the spatial distribution of the fish (Oppedal et al., 2011), and we need to make reasonable assumptions about their distribution both during and between feeding periods. For the no-feeding case, we will make the simplest possible assumption of a constant, uniform distribution β_{NF} across the full cage volume V_C:

$$\beta_{\mathrm{NF}}(x, y, z, t) = \frac{1}{V_C} \tag{6}$$

In feeding periods, the feed distribution and feed intake rates of the fish groups are calculated using the model presented by Alver et al. (2016), and we refer to that paper for the details of the feed distribution, appetite and feed ingestion models. Similarly to DO, feed density (g m^{-3}) is modelled as a spatially and temporally varying state variable $f(x, y, z, t)$. Based on the assumption that the fish, at least to some degree, follows the feed, the spatial distribution of feed ingestion is assumed to be equal to the relative distribution of the feed at any time. We can thus

define a relative distribution β_F that is proportional to the feed distribution:

$$\beta_F(x,y,z,t) = \frac{f(x,y,z,t)}{\sum_{x,y,z} f(x,y,z,t)} \quad (7)$$

Since we do not expect all fish to participate in feeding at the same time, we assume that the fish distribution in feeding periods is a combination of β_{NF} and β_F:

$$\beta\left(x,y,z,t\right) = \begin{cases} \gamma\beta_{\mathrm{NF}}(x,y,z,t) + (1-\gamma)\beta_F(x,y,z,t), & \text{if feeding,} \\ \beta_{\mathrm{NF}}(x,y,z,t), & \text{if not feeding,} \end{cases} \quad (8)$$

where γ is a parameter describing how the fish are distributed between feeding and non-feeding fish, that is set to 0.75. This assumption means that 25% of the fish are assumed to be actively feeding and hence following the feed during feeding events, while the remaining 75% follow the non-feeding distribution. We lack the detailed knowledge to estimate this parameter, but this value was chosen to reflect observations made using echosounders at OF1 indicating that a fraction of the fish tend to actively follow the feed, while the majority are found at deeper water (Myrebøe, 2019).

2.1.4. Numerical simulation

To integrate the advection-diffusion equation for the oxygen concentration $\omega(x, y, z, t)$ and feed concentration $f(x, y, z, t)$, the model domain is discretized into uniformly sized cubes with horizontal extent Δx and vertical extent Δz, and integrated using a time step Δt. The advection terms in the discrete grid are calculated using the Superbee numerical scheme to suppress numerical diffusion (e.g. Darwish and Moukalled, 2003)[1], and the diffusion terms are calculated using upstream and downstream differences as in Alver et al. (2016). The calculations for each grid cell require the values of neighbouring cells at distances of 1 and 2 cells, and for cells near the edge of the model domain, neighbouring cells outside the model domain are represented by the ambient oxygen level $\omega_A(t)$. The exception is the calculation of diffusion for the uppermost layer of cells, where values above the surface are set equal to values in the uppermost level to give a no-diffusion condition at the water surface. The model is simulated with $\Delta x = \Delta z = 2$ m, and a time step $\Delta t = 1$ s.

Preprocessing of model input values, and processing and visualization of model outputs was done using MathWorks Matlab version 2020b. The model simulation was implemented as a Java application.

Table 1
Model state variables, inputs and parameters.

Symbol	Type	Description	Value/unit
$\alpha(x, y, z, t)$	Input	Spatially distributed addition rate of oxygen	0 mg l^{-1} s^{-1}
γ	Parameter	Relative weight on non-feeding fish during feeding	0.75
k_{curr}	Parameter	Current reduction factor	0.8
$f(x, y, z, t)$	State	Feed concentration	g m^{-3}
κ_h	Parameter	Horizontal diffusion coefficient	m^2 s^{-1}
κ_v	Parameter	Vertical diffusion coefficient	m^2 s^{-1}
$\omega(x, y, z, t)$	State	3D distribution of dissolved oxygen level	mg l^{-1}
$\omega_A(t)$	Input	Ambient dissolved oxygen level	mg l^{-1}
M	Parameter	Number of weight groups of fish	7
Δt	Parameter	Simulation time step	1 s
U	Parameter	Swimming speed	1 BL s^{-1}
$v_x(t)$	Input	Eastwards component of current speed	m s^{-1}
$v_y(t)$	Input	Northwards component of current speed	m s^{-1}
W_{mean}	Input	Mean weight of fish population	g
W_{std}	Input	Standard deviation of fish weight	g
Δx	Parameter	Horizontal model resolution	2 m
Δz	Parameter	Vertical model resolution	2 m

[1] The feed distribution model based on Alver et al. (2016) has also been modified to use the Superbee scheme.

2.2. Ocean Farm 1 test cases

2.2.1. Farm properties and model configuration

The OF1 cage is shaped as a circular cylinder with a radius of 55 m and a depth of 30 m, and the model is hence set up to cover a square cuboid model domain of 112 × 112 × 30 m (Fig. 1), the cage being centered in the model domain. Each grid cell is defined as inside or outside the cage depending on whether its center lies within a 55 m radius from the center. OF1 has 16 underwater feeders placed at 6–7 m depth along four radial lines from the center at angles of 30°, 120°, 210° and 300° (angles from north, positive clockwise). Along each line, the feeders are placed approximately 19, 29, 38 and 48 m from the centre of the cage, essentially maximising the area covered. Although each group of 4 feeders in practice can be controlled independently, we chose to simplify the feeding situation in our simulations by sharing the feed input at any time equally among the 16 model cells containing the feeders.

Four oxygen sensors (CONTROS HydroFlash® O_2 optodes) are placed at 12 m depth around the outer radius of the cage, right outside the cage wall, at the same four angles as the feeders. Biofouling may affect the measurements made with the sensors, and since they could only be cleaned at specific intervals, there were variable offsets between the four sensors, complicating the comparison with model data. Since all sensors were equally likely to have offsets, we used a calibration procedure to remove offsets. For each sample time, the mean of the 20 highest measured values for each of the four sensors in a 2-day window centered on the sample time was computed. Offsets were then added to the data from each sensor at that time such that the four mean values became equal (with the four sensor offsets adding up to 0 at any time). Based on the assumption that all sensors will be positioned to measure the ambient oxygen level at some times during any 2-day period, and that the ambient oxygen level is relatively constant over this period, the offsets could then be used as reasonable correction terms that compensated for differences in calibration or fouling levels between the sensors.

We estimated ambient DO level by collecting the highest of the four calibrated measurements at any time into a time series. The time series was then low-pass filtered using a 3rd order Butterworth filter with a cut-off frequency of 3.33×10^{-4} Hz (corresponding to a period of 50 minutes) to filter out measurement noise. The filtered time series was used as the input $\omega_A(t)$ to the model. For comparison with the oxygen measurements, time series were stored of the DO concentration in the four model cells containing the sensor positions.

Current and water temperature were measured using an Acoustic Doppler Current Profiler (ADCP; Nortek AWAC 400 kHz) placed at 5 m depth right outside of the cage at an angle of 30°, near the C4 oxygen sensor. Temperature is measured at the location of the ADCP. The sensor profiles horizontally outwards from the cage, and current speeds recorded 20 m from the sensor were used as input to the model. Current speeds are generally reduced inside fish cages compared to outside speeds, so the measured current speed is multiplied by a factor $k_{curr} = 0.8$. This reduction factor is in line with previously observed values (Endresen et al., 2013; Klebert et al., 2015), but it must be noted that complex current patterns are to be expected from the interaction of the outside current, bathymetry, farm infrastructure and the influence of the fish, so the uniform current field used in the present model is a clear simplification.

2.2.2. Test cases

The cage was initially stocked in September 2017 with slightly more than 1 million smolts at a mean weight of 233 g. Since the accumulated loss of fish through the production cycle was estimated at 7% (Myrebøe,

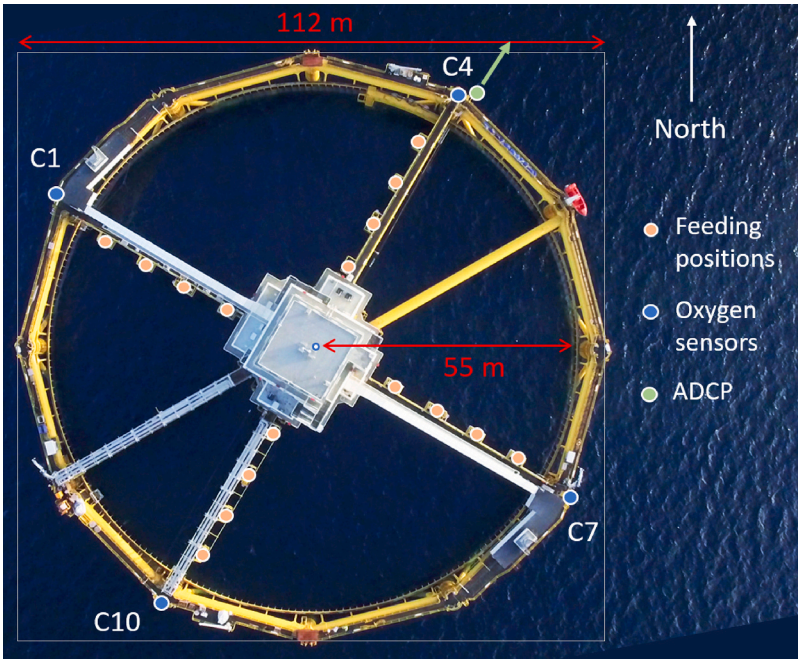

Fig. 1. Ocean Farm 1 with model domain and sensor positions indicated (photo by Salmar ASA, used with permission). The outer square indicates the extent of the model domain as seen from above. The four sensor positions (at 12 m depth) and 16 feeding positions (at 6–7 m depth) are shown along with the position of the current profiler that is pointed horizontally outwards as indicated by the arrow.

2019), we set the number of fish in the model to 1 million. The mean weight was estimated at 2540 g in June 2018, 3198 in July and 4031 in August, with a standard deviation on the order of 20%. Those values were used to configure the fish population in the model for the test case, using the 7 group distribution detailed in Table 2.

Due to the important role of water current in determining DO distribution, we ran three test cases, each lasting 48 hours representing low, moderate and high (but not extreme) current speeds at OF1:

1. Low current (8-9 June 2018). Current speeds 0.054 ± 0.028 m/s and temperatures 10.2 ± 0.2 °C.
2. Moderate current (2-3 August 2018). Current speeds 0.15 ± 0.08 m/s and temperatures 13.1 ± 0.6 °C.
3. High current (28-29 June 2018). Current speeds 0.23 ± 0.08 m/s and temperatures 10.3 ± 0.09 °C.

Temperatures and current vectors were set based on measurements in the time periods of each simulated test case. Feeding periods in the model were aligned with actual feeding periods in the corresponding test cases, with about 11–12 hours of feeding per day. The feeding rate was set to a constant level of 1.5% of the fish biomass per 12 hours of active feeding. The swimming speed was assumed to be constant at 1 BL s^{-1} (body lengths per second). We expect this to be a reasonable value, as studies have shown swimming speeds averaging from 0.2–1.9 BL s^{-1} (Juell, 1995). In a test of the critical swimming speed of salmon, it was found to be on average 2.27 BL s^{-1} (Hvas and Oppedal, 2017), and under the conditions of the test cases it is reasonable to assume that the fish are swimming significantly below critical speed.

3. Results

3.1. DO distribution within cage

Temperature and current conditions varied between the test cases, meaning that a different set of input values was used to drive the model in each simulation scenario (Fig. 2).

The 3D distribution of DO levels varies with time as a function of feeding behaviour, current conditions and temperature. See Supplementary video for a visualization of the modelled DO levels over a 15 h period from test case 1. Fig. 3 shows a single snapshot from test case 1. The time step visualised here is one where quite low modelled DO levels were encountered, at 07:20 on June 2 where there was a 0.043 m s^{-1} current straight towards the west. The fish were being fed at this time, and since the model specifies that 25% of the fish at any time follows the distribution of the feed, the drops in DO level are greatest close to the 16 feeder units. Feed was added to each of the model cells containing a feeder which are all found in the 6–8 m layer. Feed concentrations are greatest at and below feeders, so the effect of feeding is seen clearly in the '7 m' and '11 m' transects. The low current speed for this case, combined with the turbulent mixing process explains why the cells directly downstream of the feeders did not show equally low DO levels.

To illustrate typical DO levels inside the cage, Fig. 4 shows time series for all test cases at 12 m depth in the center of the cage. In all three cases, the center levels show an approximately constant baseline reduction of 0.1–0.7 mg l^{-1} compared to the ambient level, with intermittent drops of up to around 4 mg l^{-1} in test case 1, 3 mg l^{-1} in test case 2 and 0.5 mg l^{-1} in test case 3. These drops are short-term, with durations on the order of 1 hour.

Table 2
Fish group properties. *Fraction* indicates what fraction of the population is in each group. The weight of the fish in each group is W_{mean} plus W_{std} multiplied by the group's *weight deviation* value.

Group	1	2	3	4	5	6	7
Fraction	0.0228	0.1359	0.2120	0.2586	0.2120	0.1359	0.0228
Weight deviation	-2.36	-1.37	-0.63	0	0.63	1.37	2.36

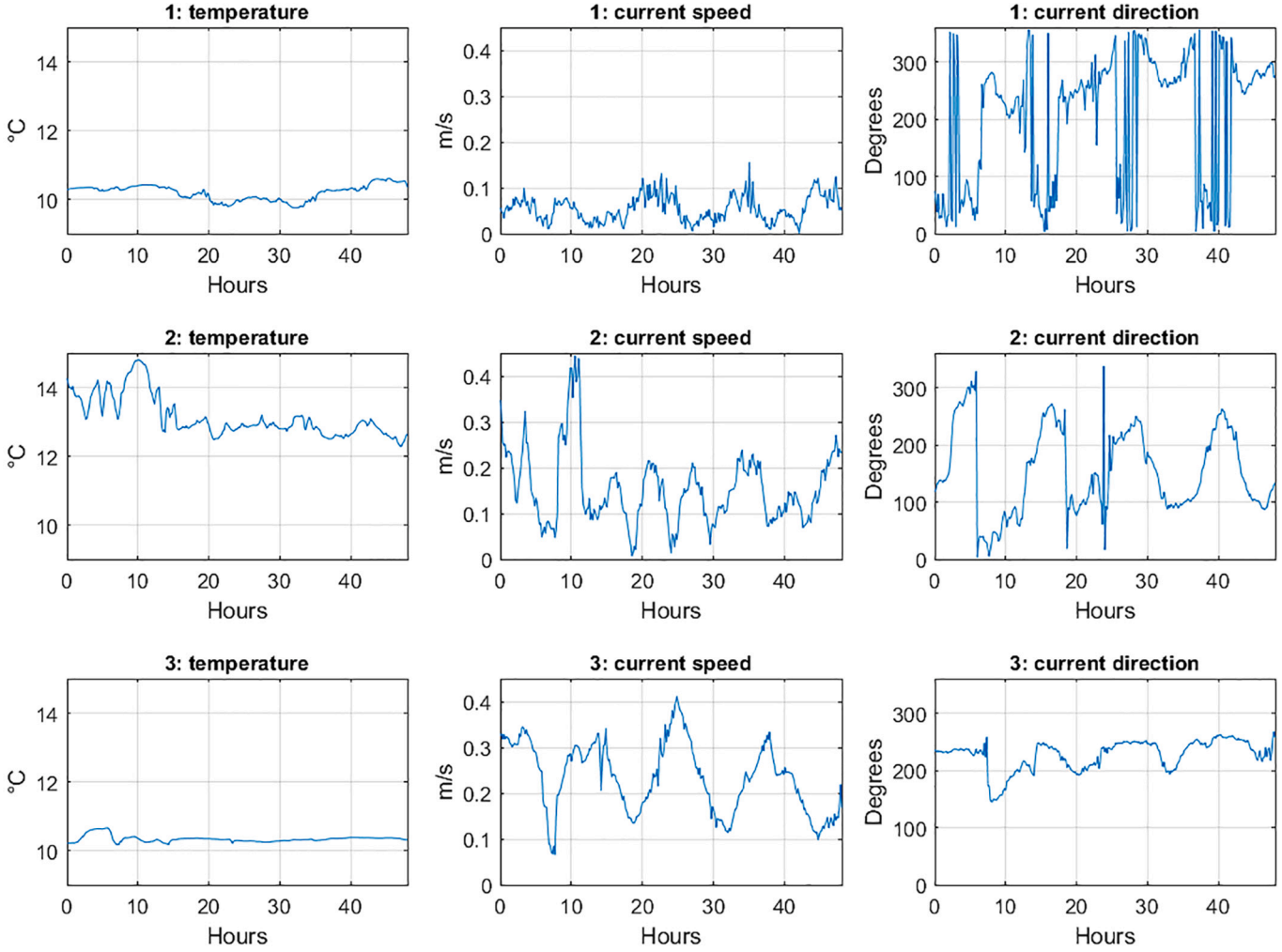

Fig. 2. Temperature and current in the three test cases. Current directions are defined positive clockwise, with 0° indicating current to the north.

3.2. Comparison between model and measurements

Test case 1 represents a low current speed scenario, and both the model and the observations show regular clear drops in DO concentrations (Fig. 5) coinciding with the times when current speeds were at their lowest due to the tidal cycle. The saturation concentration in this period was around 9.0–9.4 mg l^{-1}, and the observed drops were frequently down to below 7.5 mg l^{-1} at the sensor positions. The modelled reductions in concentration (ambient level minus level at sensor position) are positively correlated with observed reductions, and standard deviations between observed and modelled values are on the order of 0.5 mg l^{-1} (Table 3). We also see that the observed statistical distribution of DO values are well reproduced by the model (Fig. 8).

Test case 2 represents moderate, but quite variable, current speeds. At C1, very small drops in DO level were observed, while the model predicts a few larger drops of around 0.5 mg l^{-1} (Fig. 6). At C4, one large drop that was partly reproduced by the model was observed early in the period. Values constantly 0.2–0.3 mg l^{-1} below ambient levels were measured at C4 for the second half of the period, a deviation that was not seen in the model results. At C7 and C10, regular drops of 1.0–1.5 mg l^{-1} were seen, and the model reproduced most of these fully or partly. Oxygen reductions seen in the model output were uncorrelated with observed reductions at C1, but positively correlated at the other locations, and standard deviations between observed and modelled values were in the range 0.24–0.48 mg l^{-1} (Table 3). The statistical distribution of DO values featured lower values in the model than observed at C1, a slight positive bias in the model at C4, showed the model not reproducing the lower range of the distribution at C7, and fairly good agreement with a slight bias toward ambient levels in the model at C10.

Test case 3 represents high current speeds, and the current direction was towards the south-west quadrant throughout the period. Observed DO level drops were within 0.3 mg l^{-1} at all sensor locations, the largest occurring at C1 and C7, and the smallest at C10. The model generally estimated DO drops comparable to observations at C1, and predicted generally smaller drops and lower variations than the observations at C4 and C7. At C10, the model predicted drops of up to 1.0 mg l^{-1}, which was higher than the observed drops. These deviations are seen also in the statistical distributions (Fig. 8), but it should be noted that the standard deviations are fairly small (around 0.1 mg l^{-1}) due to the small range of DO level variation in this period (Table 3).

The DO sensors at OF1 are placed pairwise at opposing sides of the cage, providing an opportunity to track the differential DO levels upstream and downstream. Through the time spans of the three test cases the current direction varies, so different sensors are closest to the upstream direction at different times. Fig. 9 shows modelled and observed differentials, with color codings used to indicate periods when the current direction is in the two quadrants along the axis of the sensor pair. It is clear in all test cases that the model produces differentials in the expected directions when the current goes along the sensor axes. This is the case most of the time in the observed differentials in test cases 1 and 2 as

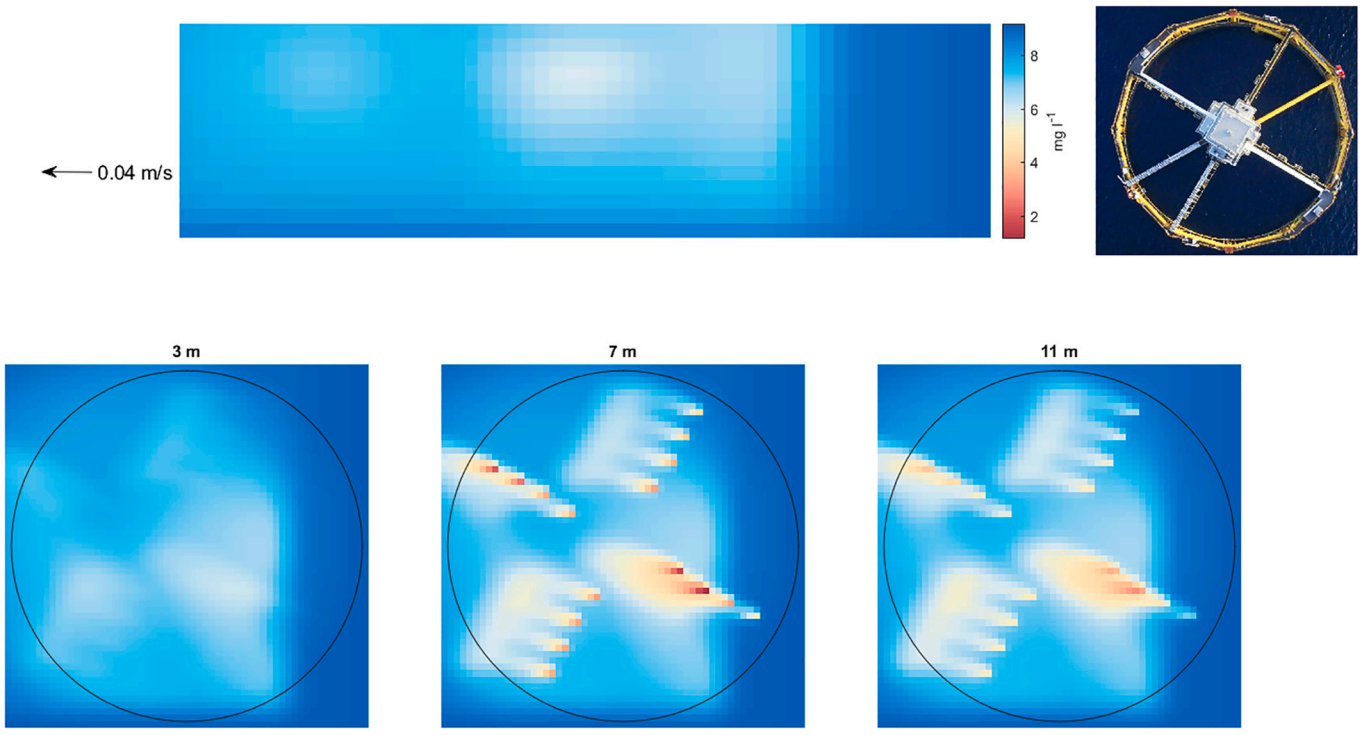

Fig. 3. Model transects at 8 June 07:20. The current speed was 0.04 m s^{-1} directly towards the west, as indicated by the arrow. Top center: vertical west-east transect through center of cage. Top right: OF1 seen from above (photo by Salmar ASA, used with permission), oriented with north upwards. Bottom: three horizontal transects at different depths, oriented with north upwards. Circles indicate the extent of the cage. The same color scale is used in all transects. The 16 feeders, which are active at the time of the snapshot, are at 6–7 m depth.

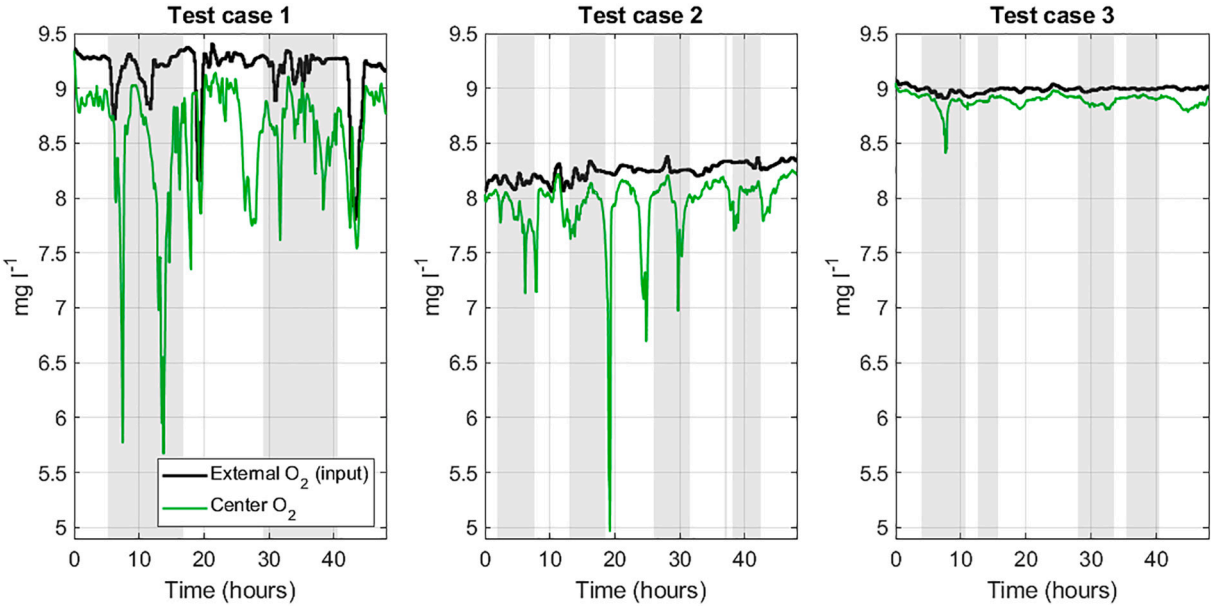

Fig. 4. Time series of modelled DO value at 12 m depth in the centre of the cage. The estimated ambient DO value that is used as input to the model is shown (black lines) along with modelled values (green lines) Gray vertical bars indicate feeding periods. (For interpretation of the references to color in this figure legend, the reader is referred to the web version of this article.).

well. In test case 3, where the current direction is most of the time towards the south west quadrant, the observed C4-C10 differential does not show the expected values.

4. Discussion

4.1. Model performance

The agreement between the statistical distribution of DO values from the model output and measurements was fairly good for all three cases,

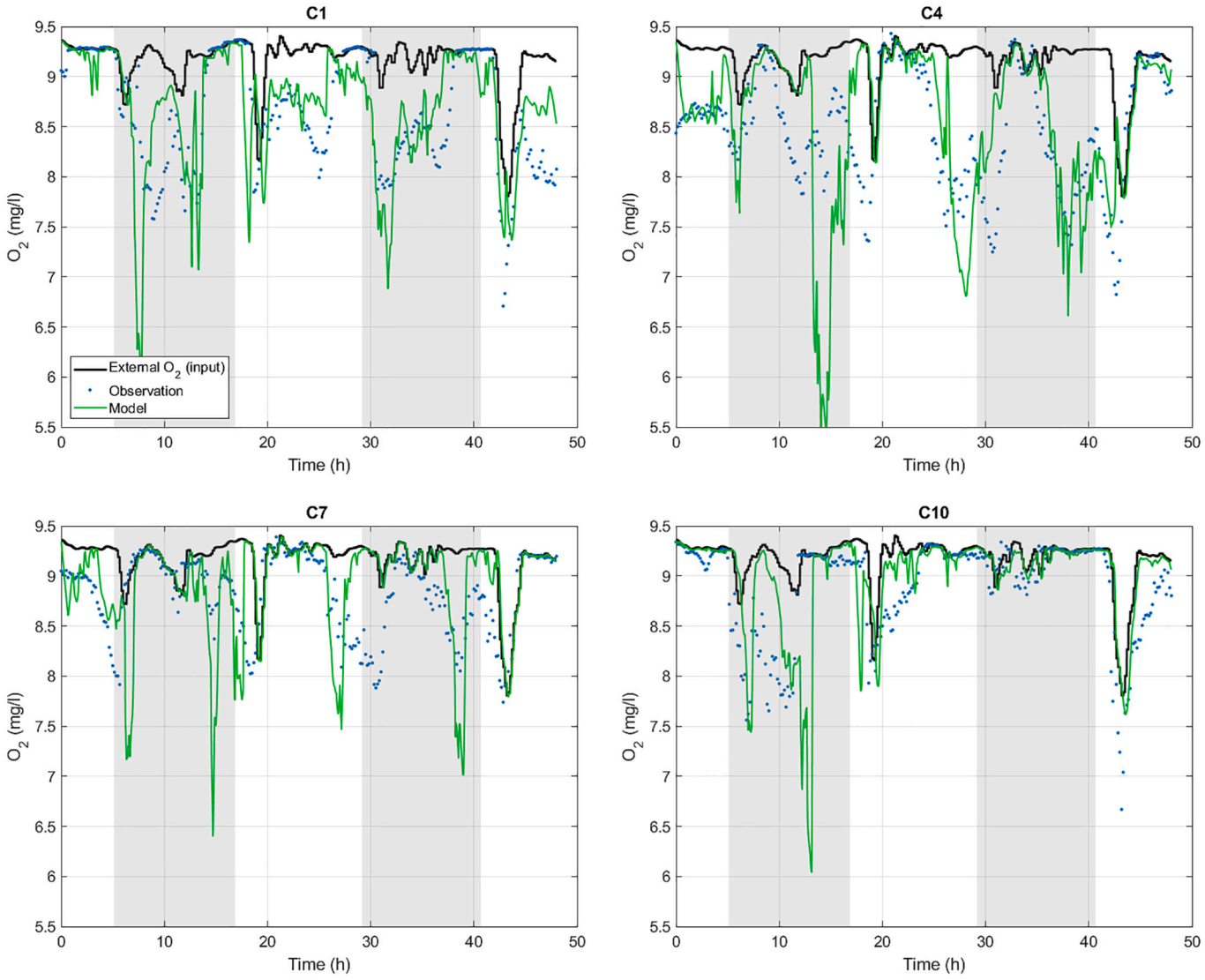

Fig. 5. DO levels in test case 1 (8–9 June 2018) at the four sensor positions (at 12 m depth). The estimated ambient DO value that is used as input to the model is shown (black lines) along with observations (blue dots) and modelled values at the sensor positions (green lines). Gray vertical bars indicate feeding periods. (For interpretation of the references to color in this figure legend, the reader is referred to the web version of this article.)

Table 3
Correlation coefficients and standard deviations (mg l^{-1}) between measured and modelled reductions in DO levels at sensor positions. The statistics are computed based on the difference between estimated ambient DO levels and observed and modelled levels, respectively.

Test case	C1		C4		C7		C10	
Statistic	Corr	Std	Corr	Std	Corr	Std	Corr	Std.
1. Low current	0.51	0.52	0.51	0.71	0.32	0.53	0.23	0.53
2. Moderate current	-0.04	0.24	0.71	0.29	0.44	0.48	0.56	0.38
3. High current	0.41	0.10	0.29	0.050	0.61	0.075	-0.12	0.11

implying that the model was able to capture the main dynamics in the system. This is despite the model not having information about the distribution of the fish beyond the simple assumptions built into the model. The actual distribution of fish at any time can be affected by feeding, light conditions, temperature, currents, waves and other events, salmon lice loads and the health condition of the fish, and will have an impact on the DO levels measured at the four sensor positions. As seen in the test cases, the model agreed well with observations in the low current speed case, had more variable match with measurements in the moderate current case, and deviated most from observed data in the high current case (Figs. 5–7). This may further indicate that the model was better at reflecting system dynamics when current levels are low, and hence that the impact of eventual modelling errors were most pronounced for higher currents. This was also evident in the differential values (Fig. 9), where the observations showed values along the C4–C10 axis that would not be expected based on the measured current direction. It can be noted that the risk of hypoxia is mostly an issue at low current speeds, which makes the model's performance at high current speeds less concerning.

One of the main sources of model inaccuracies in this study was probably the very simplified representation of the current conditions within a fish cage. The flow field was modelled using a uniform current

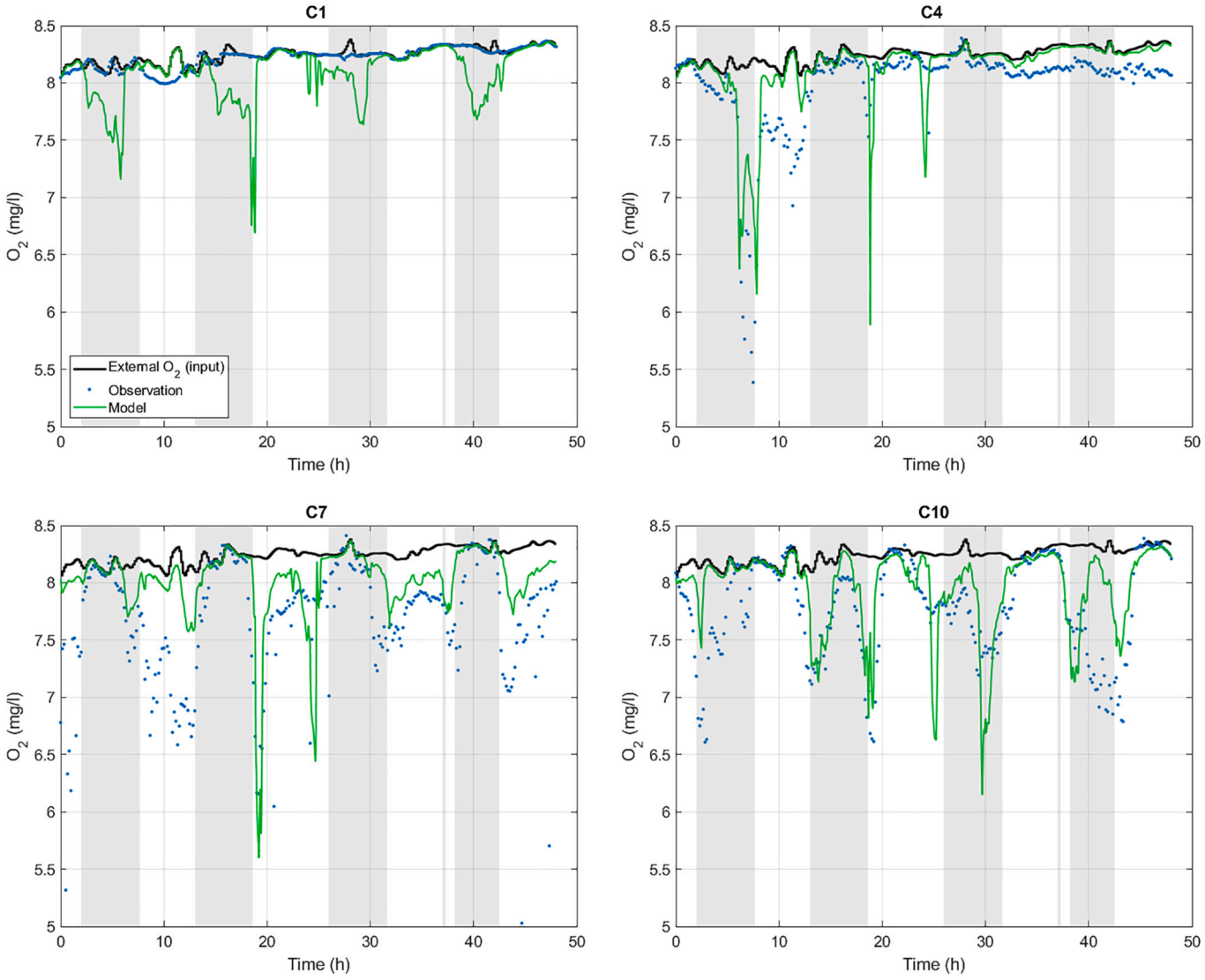

Fig. 6. DO levels in test case 2 (2–3 August 2018) at the four sensor positions (at 12 m depth). The estimated ambient DO value that is used as input to the model is shown (black lines) along with observations (blue dots) and modelled values at the sensor positions (green lines). Gray vertical bars indicate feeding periods. (For interpretation of the references to color in this figure legend, the reader is referred to the web version of this article.)

field based on a single point measurement, coupled with uniform turbulent mixing. This is likely to be more appropriate simplification at low current speeds than at high speeds, as turbulent interactions between the flow field outside the cage, and the cage itself and the fish will become more pronounced at high speeds. The model assumes that an oxygen sensor in a downstream position will mostly see water that has passed through the cage, while in reality the sensor may see a mix also with water that has passed around the cage due to the complex flow field (Klebert et al., 2013). In addition, the fish may be distributed differently as they swim directly against the current at high current speeds (Johansson et al., 2014), thereby influencing the spatial distribution of oxygen consumption. These factors may explain why the model agrees better with measurements at low current speeds than at high speeds, although speeds may not have been high enough in any of the test cases to make the fish switch to swimming against the current.

Another possible explanation for the observed deviations is linked to how farm operation was portrayed in the model. In particular, feeding was assumed to be evenly distributed between the 16 feeding points. This is not likely to be true in all cases, and particularly under strong currents, feeding is likely to be biased towards upstream feeding points to reduce feed wastage. The operators at OF1 can adjust the percentage of feed that goes into each quadrant (each with 4 feeders), but cannot control each feeder individually. In test case 3 (i.e. with the strongest current levels), the current direction is predominantly toward the south west, indicating that feeding should be biased toward the north-eastern part of the cage. To test this, we ran a short test simulation with the model where the feeders in the south-west quadrant were disabled and the feed was distributed evenly between the remaining 12 feeding points. This resulted in a somewhat better match at C10, with slightly reduced drops in DO level. However, although this partly explains the large deviations at C10, the effect seems too small for this to be the sole explanation for the discrepancy.

We also see events in the test cases where the measurements show markedly larger or smaller drops in DO level than those predicted by the model. These events cannot be tied to either feeding or non-feeding periods, but occur in both cases, and are also reflected in the statistical distributions of DO levels seen in the test cases, although the distributions overall correspond reasonably well to observed values. These deviations were most likely caused by inaccurate representations of either the fish distribution or the current conditions at the sites. The predictions in these cases would most likely have been improved if the model had access to detailed information about the fish distribution and

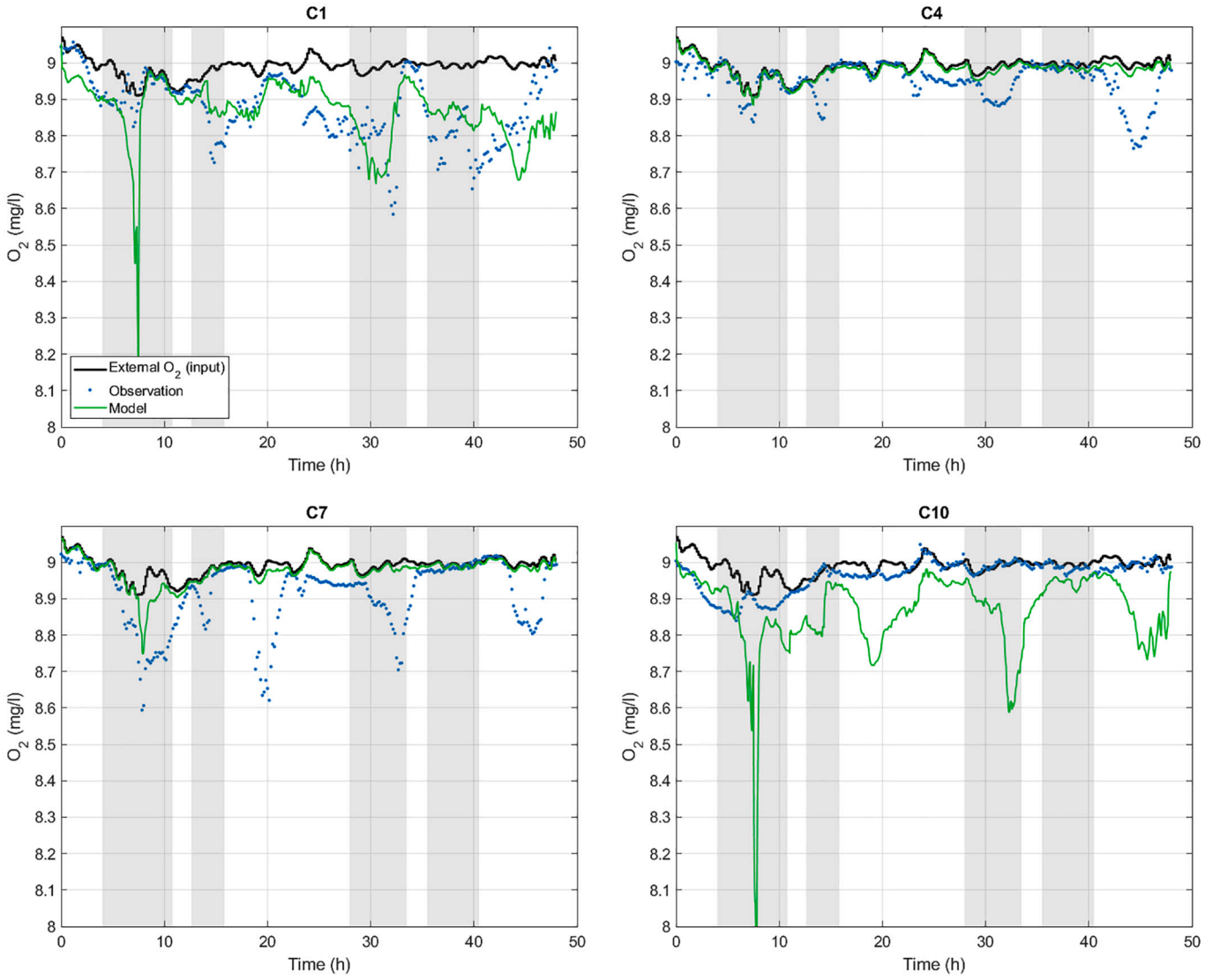

Fig. 7. DO levels in test case 3 (28–29 June 2018) at the four sensor positions (at 12 m depth). The estimated ambient DO value that is used as input to the model is shown (black lines) along with observations (blue dots) and modelled values at the sensor positions (green lines). Gray vertical bars indicate feeding periods. (For interpretation of the references to color in this figure legend, the reader is referred to the web version of this article.)

current conditions.

4.2. Uncertainty and model limitations

The calibration procedure for removing offsets between oxygen sensors is associated with uncertainties that may have resulted in incorrect offsets. Since the bias was intended to compensate for the effects of differential fouling between the sensors, this would be particularly relevant in cases where the average bias across sensors is different from 0. As the procedure computes offsets that always sum up to 0, in this situation the original bias would not be removed. The estimated offsets vary slowly and the offsets are thus approximately constant within each test case. This effect therefore does not significantly affect the relative variations between and within the datasets from the individual sensors within each test case. However, it does render the method of estimating the ambient DO level based on the highest sensor value at each time more uncertain, and may have given too-low values in cases where none of the sensors experienced water unaffected by the oxygen consumption within the cage. The ambient values would also be under- or overestimated if the average bias of the sensors was significantly different from 0, but this would not hinder comparison between the model and observations since the same bias would apply to both.

If the water column is stratified, both ambient DO level, current speed, temperature and mixing properties may be depth dependent. In the current setup, the model uses single depth measurements of DO level, temperature and current as if they were valid for all model depths. It is straightforward to utilize measurements at multiple depths in the model, and under stratified conditions this can contribute towards improving the model accuracy. For OF1, temperatures at 5 m and 15 m were recorded for a full year in 2018 (Myrebøe, 2019), showing small differences except in the summer when differences of 0.5–2.0 ° C were seen due to solar input heating up the upper water column. The temperature measured at 5 m may therefore overestimate the temperature deeper down in the cage. We tested the model's sensitivity by running test case 1 with 2 ° C lower temperature, and this lead to very small changes in DO levels observed at the sensor positions. The largest differences coincided with the strongest DO level drops, where the lowered temperature reduced the extent of the drops by up to 0.2 mg l^{-1}.

The discretization of the model implies that any model estimate represents the average concentration in a $2 \times 2 \times 2$ m cell. Any variability in DO level at smaller scales than this cannot be represented by the model unless its resolution is increased, and would hence be

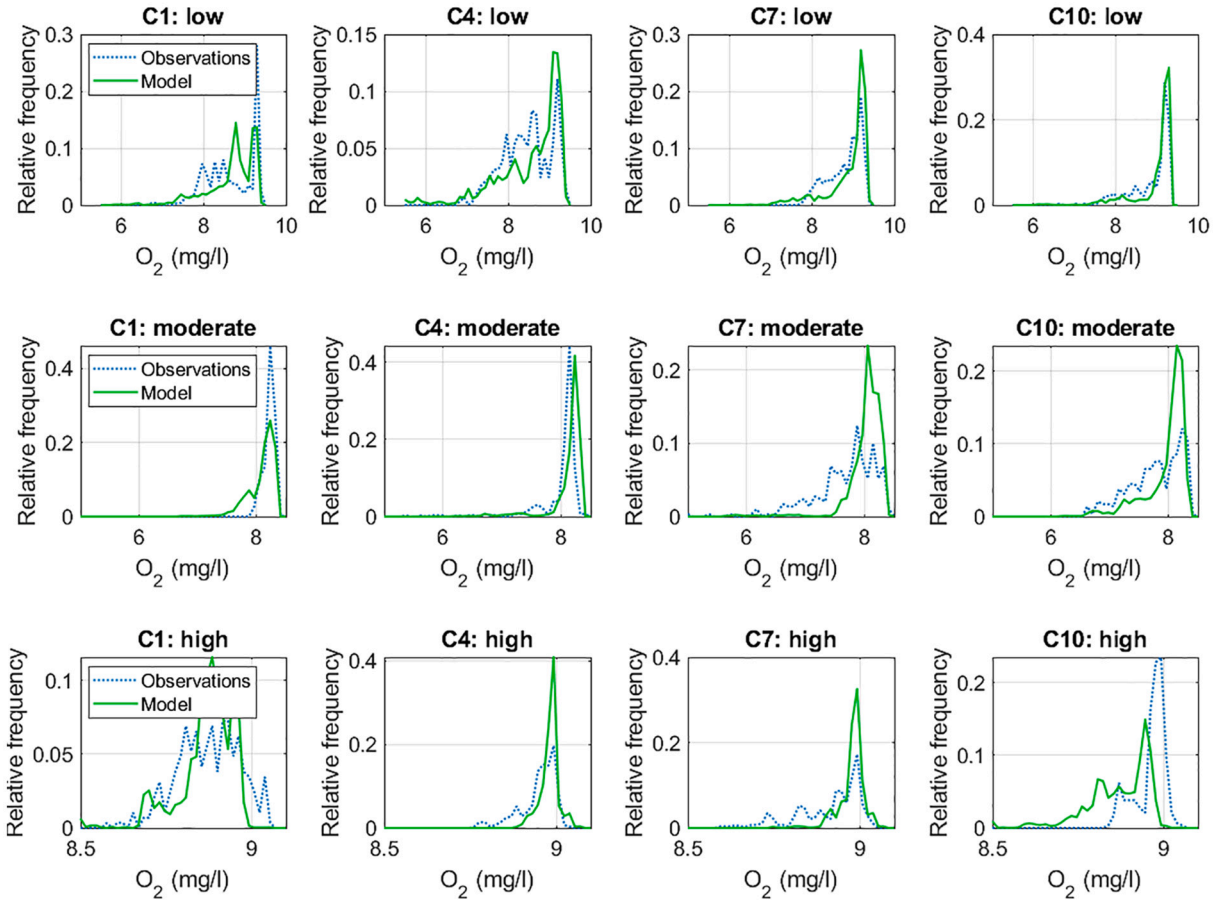

Fig. 8. Relative distribution of DO values occurring at the four sensor positions for all test cases. Note that the *x* axis is different for the three test cases, reflecting different ranges of DO values seen.

impossible for the model to capture. Although this could potentially affect comparisons with sensor outputs that correspond to point locations, we do not believe that this has significantly affected the deviations seen between the model and observations in our studies. Increasing the resolution to 1 m results in a 16 times increase in the model's computational load since the time step must then be halved while the number of cells increases by a factor of 8. We explored the effect of this through a simple test simulation, the outcomes of which showed that this change had very little effect on the modelled DO levels at the sensor locations, indicating that a 2 m resolution is sufficient for the OF1 scenario. It is possible that similar simulation studies focused on conventional cages or smaller volumes would require a higher resolution to yield realistic outcomes, but the spatial domain covered by the model would then be correspondingly smaller, cancelling out some of the increased computational load due to smaller grid cells.

A factor that affects oxygen consumption rate is the digestion of feed. According to Forsberg (1997), the energy expenditure for digestion and transportation of feed may be a major determinant of the oxygen consumption in fish. In the study of Grøttum and Sigholt (1998), the fish were not fed for 24 hours before the start of the experiment, so digestion activity is not contributing to the consumption rates predicted by their model. For the present model, this is likely to mean that oxygen consumption is underestimated. The effect of digestion activity could be addressed by estimating increased consumption rate by taking the actual digestion rate into account, since feed ingestion and gut evacuation as modelled in Alver et al. (2004, 2016) is also included in our model.

The swimming speed U used in the calculation of oxygen consumption was kept constant, even though it would be reasonable to assume elevated swimming speeds when the fish are feeding actively (Oppedal et al., 2011). Increasing the value of U during feeding in the model simulations would lead to greater estimated oxygen consumption in these periods. However, since it is likely that only a fraction of the fish are actively feeding at the same time, an effect we account for in the spatial distribution of fish in the simulations, a smaller increase in U than that typically assumed during feeding might be more realistic. Although individual based or statistical data on fish feeding behaviour could be used to improve this aspect of the model, there exist few published studies that quantify how feeding affects the swimming speeds of salmon during feeding.

The model neglects the interchange of oxygen across the ocean surface. In reality, whenever the DO level in surface waters is below saturation, there will be a replenishment from the air above the surface. However, the water within a fish cage is replaced in a matter of minutes, or up to an hour at very slow current speeds in a large unit such as OF1. Given also the high rate of oxygen consumption at high fish densities, the slow replenishment process is not likely to significantly affect the DO values within the cage (Wildish et al., 2021). Oxygen supply through photosynthesis by microalgae within the cage is also neglected in the model, as the production rate is expected to be very slow compared to the oxygen consumption rate within a fish cage (Wildish et al., 2021).

4.3. Model applications and further work

The simulation scenarios tested in this work uses measurement of external current speed and estimated measurement of ambient DO level along with information about the fish biomass, the feeding input and the geometry of the cage to provide 3D estimates of DO levels in a cage volume. This information can be acquired in real time for any sea cage

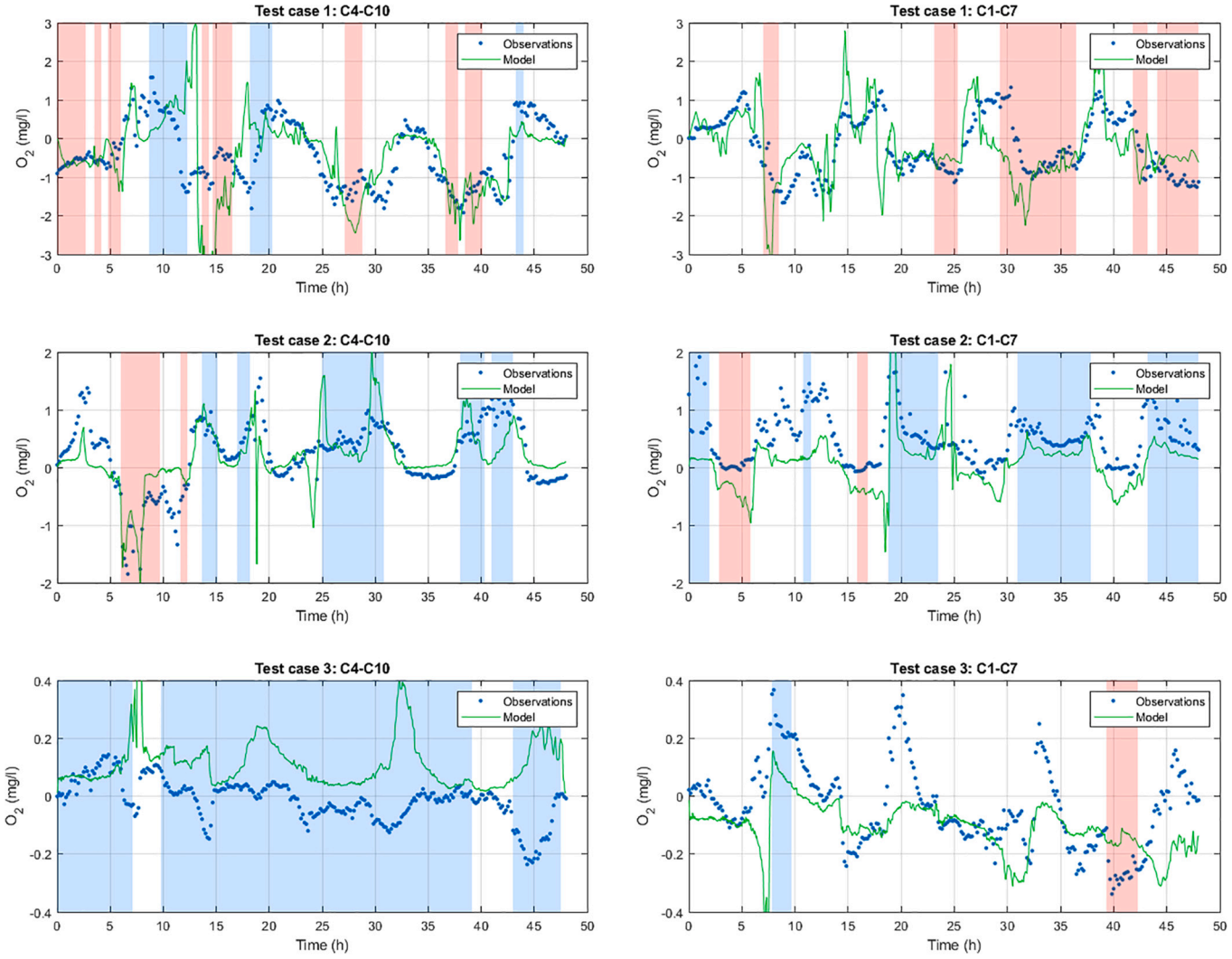

Fig. 9. Differences in DO levels measured by sensors on opposing sides in all test cases. Red and blue vertical bars indicate periods with current directions in quadrants along the sensor axes. Left panels: red indicates current directions in the interval [− 15, 75], and blue in the interval [165, 255]. Right panels: red indicates current directions in the interval [255, 345], and blue in the interval [75, 165]. Intervals are chosen so negative values are expected in red periods, and positive values in blue periods. (For interpretation of the references to color in this figure legend, the reader is referred to the web version of this article.)

with moderate investments, and lets the model produce reasonably reliable estimates of the immediate risk and extent of hypoxic conditions in the cage. Since current speeds also can be forecast, the model can also be used to forecast the short-term risk of hypoxic conditions so appropriate precautions can be taken. The model would then need to be combined with or receive inputs from an oceanographic model.

For the test cases studied in this work, there are occurrences of low DO levels, particularly near the feeding positions. The local minima found at the feeding positions are hard to reliably quantify as the values are sensitive to the model's assumptions of fish behaviour and turbulent diffusion coefficients. We can more reliably quantify the fraction of the cage volume that shows low DO levels. If we set a threshold at 5 mg l^{-1}, values below the threshold occurred in a maximum of 3.3 and 2.3 % of the cage volume in test cases 1 and 2, respectively. No values below the threshold were seen more than 91 and 98 % of the time in test cases 1 and 2, respectively. No values below the threshold were seen in test case 3. These numbers are merely indications, and should not be used to evaluate DO conditions in general at OF1.

As discussed in Section 4.1, the application of more sophisticated inputs would likely improve the precision of the model. For instance, Computational Fluid Dynamics (CFD) model studies can be used to compute more representative current speeds and directions and turbulent mixing coefficients around and within the cage, which in turn can be directly applied in the present model. Moreover, more detailed knowledge about fish behaviour in various situations and under different current conditions could be incorporated into the model to achieve a more representative and realistic spatial distribution of oxygen consumption. This could be achieved when echosounders are used to monitor the distribution of the fish, as in OF1, by using processed data from these as inputs into the model in real-time to account for the actual distribution of the fish.

Aside from the operational use of the model, it can, in combination with CFD studies, serve as a tool to evaluate the oxygen conditions in various different production systems, including open, semi-closed and closed. Simulations showing the range of plausible environmental conditions as well as different system design parameters could be used to test system designs to ensure acceptable fish welfare with regard to oxygen levels prior to their physical construction.

Supplementary data to this article can be found online at https://doi.org/10.1016/j.aquaculture.2021.737720.

Declaration of Competing Interest

The authors declare that they have no known competing financial

interests or personal relationships that could have appeared to influence the work reported in this paper.

Acknowledgements

We would like to thank Salmar Ocean AS for granting access to the observational data from Ocean Farm 1, and Berit F. Lund at Kongsberg Maritime for extracting the relevant data series and providing the necessary information about the technical installations at OF1, as well as for useful discussions and input to this study.

References

Alver, M.O., Alfredsen, J.A., Sigholt, T., 2004. Dynamic modelling of pellet distribution in Atlantic salmon (*Salmo salar* L.) cages. Aquac. Eng. 31, 51–72. https://doi.org/10.1016/j.aquaeng.2004.01.002.

Alver, M.O., Skøien, K.R., Føre, M., Aas, T.S., Oehme, M., Alfredsen, J.A., 2016. Modelling of surface and 3d pellet distribution in Atlantic salmon (Salmo salar l.) cages. Aquac. Eng. 72, 20–29. https://doi.org/10.1016/j.aquaeng.2016.03.003.

Burt, K., Hamoutene, D., Mabrouk, G., Lang, C., Puestow, T., Drover, D., Losier, R., Page, F., 2012. Environmental conditions and occurrence of hypoxia within production cages of Atlantic salmon on the south coast of newfoundland. Aquac. Res. 43, 607–620. https://doi.org/10.1111/j.1365-2109.2011.02867.x.

Darwish, M.S., Moukalled, F., 2003. Tvd schemes for unstructured grids. Int. J. Heat Mass Transf. 46, 599–611. https://doi.org/10.1016/S0017-9310(02)00330-7.

Endresen, P.C., Føre, M., Fredheim, A., Kristiansen, D., Enerhaug, B., 2013. Numerical modeling of wake effect on aquaculture nets. In: Proceedings of the ASME 2013 32nd International Conference on Ocean, Offshore and Arctic Engineering. Volume 3: Materials Technology; Ocean Space Utilization. https://doi.org/10.1115/OMAE2013-11446.

Forsberg, O., 1997. The impact of varying feeding regimes on oxygen consumption and excretion of carbon dioxide and nitrogen in post-smolt Atlantic salmon Salmo salar l. Aquac. Res. 28, 29–41. https://doi.org/10.1046/j.1365-2109.1997.00826.x.

Grøttum, J.A., Sigholt, T., 1998. A model for oxygen consumption of Atlantic salmon (Salmo salar) based on measurements of individual fish in a tunnel respirometer. Aquac. Eng. 17, 241–251. https://doi.org/10.1016/S0144-8609(98)00012-0.

Hvas, M., Oppedal, F., 2017. Sustained swimming capacity of Atlantic salmon. Aquac. Environ. Interact. 9, 361–369. https://doi.org/10.3354/aei00239.

Johansson, D., Juell, J.E., Oppedal, F., Stiansen, J.E., Ruohonen, K., 2007. The influence of the pycnocline and cage resistance on current flow, oxygen flux and swimming behaviour of Atlantic salmon (Salmo salar l.) in production cages. Aquaculture 265, 271–287. https://doi.org/10.1016/j.aquaculture.2006.12.047.

Johansson, D., Laursen, F., Fernö, A., Fosseidengen, J.E., Klebert, P., Stien, L.H., Vågseth, T., Oppedal, F., 2014. The interaction between water currents and salmon swimming behaviour in sea cages. PloS one 9, e97635. https://doi.org/10.1371/journal.pone.0097635.

Johansson, D., Ruohonen, K., Kiessling, A., Oppedal, F., Stiansen, J.E., Kelly, M., Juell, J. E., 2006. Effect of environmental factors on swimming depth preferences of Atlantic salmon (Salmo salar l.) and temporal and spatial variations in oxygen levels in sea cages at a fjord site. Aquaculture 254, 594–605. https://doi.org/10.1016/j.aquaculture.2005.10.029.

Jónsdóttir, K.E., Volent, Z., Alfredsen, J.A., 2021. Current flow and dissolved oxygen in a full-scale stocked fish-cage with and without lice shielding skirts. Appl. Ocean Res. 108, 102509. https://doi.org/10.1016/j.apor.2020.102509.

Juell, J.E., 1995. The behaviour of Atlantic salmon in relation to efficient cage-rearing. Rev. Fish Biol. Fish. 5, 320–335.

Klebert, P., Lader, P., Gansel, L., Oppedal, F., 2013. Hydrodynamic interactions on net panel and aquaculture fish cages: a review. Ocean Eng. 58, 260–274. https://doi.org/10.1016/j.oceaneng.2012.11.006.

Klebert, P., Patursson, Ø., Endresen, P.C., Rundtop, P., Birkevold, J., Rasmussen, H.W., 2015. Three-dimensional deformation of a large circular flexible sea cage in high currents: field experiment and modeling. Ocean Eng. 104, 511–520. https://doi.org/10.1016/j.oceaneng.2015.04.045.

Myrebøe, G., 2019. Sluttrapport Prosjekt Ocean Farm 1. Technical Report. Ocean Farming. URL: https://www.fiskeridir.no/Akvakultur/Tildeling-og-tillatelser/Saerti llatelser/Utviklingstillatelser/Kunnskap-fra-utviklingsprosjektene. in Norwegian.

Oldham, T., Oppedal, F., Dempster, T., 2018. Cage size affects dissolved oxygen distribution in salmon aquaculture. Aquacult. Environ. Interact 10, 149–156. https://doi.org/10.3354/aei00263.

Oppedal, F., Dempster, T., Stien, L.H., 2011. Environmental drivers of atlantic salmon behaviour in sea-cages: a review. Aquaculture 311, 1–18. https://doi.org/10.1016/j.aquaculture.2010.11.020.

Remen, M., Oppedal, F., Imsland, A.K., Olsen, R.E., Torgersen, T., 2013. Hypoxia tolerance thresholds for post-smolt atlantic salmon: dependency of temperature and hypoxia acclimation. Aquaculture 416-417, 41–47. https://doi.org/10.1016/j.aquaculture.2013.08.024.

Remen, M., Sievers, M., Torgersen, T., Oppedal, F., 2016. The oxygen threshold for maximal feed intake of atlantic salmon post-smolts is highly temperature-dependent. Aquaculture 464, 582–592. https://doi.org/10.1016/j.aquaculture.2016.07.037.

Smagorinsky, J., 1963. General circulation experiments with the primitive equations: I. the basic experiment. Month. Weather Rev. 91, 99–164 doi:10.1175/1520-0493(1963)091<0099:GCEWTP>2.3.CO;2.

Solstorm, D., Oldham, T., Solstorm, F., Klebert, P., Stien, L.H., Vågseth, T., Oppedal, F., 2018. Dissolved oxygen variability in a commercial sea-cage exposes farmed Atlantic salmon to growth limiting conditions. Aquaculture 486, 122–129. https://doi.org/10.1016/j.aquaculture.2017.12.008.

Wildish, D.J., Keizer, P.D., Wilson, A.J., Martin, J.L., 2021. Seasonal changes of dissolved oxygen and plant nutrients in seawater near salmonid net pens in the macrotidal bay of fundy. Can. J. Fish. Aquat. Sci. 50, 303–311. https://doi.org/10.1139/f93-035.